Automated aortic anatomy analysis: From image to clinical indicators

Mounir Lahlouh, Yasmina Chenoune, Raphaël Blanc, Michel Piotin, Simon Escalard, Robert Fahed, Jérome Szewczyk, Nicolas Passat

Automated Aortic Anatomy Analysis: from Image to Clinical Indicators

M. Lahlouh, Y. Chenoune, R. Blanc, M. Piotin, S. Escalard, R. Fahed, J. Szewczyk and N. Passat*

***Abstract*— Most cerebrovascular diseases (including strokes and aneurysms) are treated endovascularly with catheters that are navigated from the groin through the vessels to the brain. Many patients have complex anatomy of the aortic arch and supra-aortic vessels, which can make it difficult to select the best catheters for navigation, resulting in longer procedures and more complications or failures. To this end, we propose a framework dedicated to the analysis of the aortic arch and supra-aortic trunks. This framework can automatically compute anatomical and geometrical features from meshes segmented beforehand via CNN-based pipeline. These features such as arch type, tortuosity and angulations describe the navigational difficulties encountered during catheterization. Quantitative and qualitative validation was performed by experienced neuroradiologists, leading to reliable vessel characterization.**

***Clinical relevance*— This method allows clinicians to determine the type and the anatomy of the aortic arch and its supra-aortic trunks before endovascular procedures. This is essential in interventional neuroradiology, such as navigation with catheters in this complex area.**

***Keywords*— Aortic arch, vascular anatomy, segmentation, geometrical features, magnetic resonance angiography.**

I. INTRODUCTION

According to World Health Organization 2019 report, stroke is the second leading cause of death worldwide[1]. In France, the National Institute of Statistics and Economic Studies reports that neurovascular diseases are the second most common cause of death for men and remain the leading one for women in 2017[2]. Besides, they are a frequent cause of hospitalization and disability.

Neurovascular pathologies such as aneurysms, arterial stenosis, or arteriovenous malformations are mainly treated by endovascular procedures, e.g. embolization, mechanical thrombectomy or stenting. These procedures are minimally invasive; neuroradiologists access arteries using long and flexible guides called catheters. Catheterization is a technical procedure that highly depends on the physician experience facing challenging vascular morphologies. Besides, some diseases are time sensitive (such as stroke) and treatments need to be performed as fast as possible, as each delay increases risk of poor outcomes. The duration of the procedure mainly depends on the time during which they torque and exchange catheters. In particular, changing catheters during the intervention increases the risk of infection, injury and radiation exposure time. As a consequence, optimizing the intervention time is important. In this context, many studies proved that navigation difficulty and prevalence of neurovascular diseases is strongly correlated with the anatomy of vascular structures.

The first anatomical constraints that the catheter encounters when navigating to the brain are related to the aortic arch morphology. This anatomical structure is challenging due to its inter-patient variability. Indeed, the aortic arch is commonly classified into three types (I, II and III) [1] (Fig. 1). Each type has its own anatomical characteristics, that induce clinical implications in endovascular interventions.

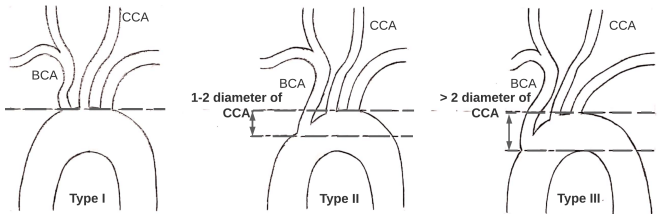

Fig. 1. Madhwal aortic arch anatomy classification [1]. Type I: the vertical distance from the top of the aortic arch to the origin of the brachiocephalic artery (BCA) is lower than the left common carotid artery (CCA) diameter. Type II: this distance is between 1 and 2 times CCA diameter. Type III: this distance is more than 2 times CCA diameter.

In carotid artery stenting (CAS), many studies [2], [3] show that adverse aortic arch anatomies are associated with longer intervention times. In particular, it was observed that type III arches, due to their elongated anatomy and the increased tortuosity of their supra-aortic trunks, extend the catheter manipulation time (CMT) and jeopardize the success

*This work was financially supported by BCV, a French medtech company developing solutions to enhance endovascular navigation, and by the French *Association Nationale de la Recherche et de la Technologie* (ANRT) (grant 2020/0638).

Mounir Lahlouh is with CReSTIC, Université de Reims Champagne Ardenne, Reims, France, ESME Sudria Research Lab, Paris, France and BCV, Paris, France mounir.lahlouh@esme.fr

Yasmina Chenoune is with ESME Sudria Research Lab, Paris, France and LISSI, Université Paris-Est, Vitry-sur-Seine, France yasmina.chenoune@esme.fr

Raphaël Blanc, Michel Piotin and Simon Escalard are with Fondation Ophtalmologique de Rothschild, Interventional Neuroradiology Department, Paris, France {rblanc, mpiotin, sescalard}@for.paris

Robert Fahed is with Department of Medicine, Division of Neurology, The Ottawa Hospital, Ottawa Hospital Research Institute, University of Ottawa, Ottawa, Ontario, Canada and with Fondation Ophtalmologique de Rothschild, Interventional Neuroradiology Department, Paris, France rfahed@toh.ca

Jérôme Szewczyk is with ISIR, Sorbonne Université, Paris, France sz@isir.upmc.fr

Nicolas Passat is with CReSTIC, Université de Reims Champagne Ardenne, Reims, France nicolas.passat@univ-reims.fr

M. Lahlouh is funded by BCV. R. Blanc and J. Szewczyk are founders of BCV.

[1]https://www.who.int/news-room/fact-sheets/detail/the-top-10-causes-of-death

[2]https://www.insee.fr/en/outil-interactif/5543645/tableau/40_SOC/45_SHD

of the procedure. It was also proven that this type of arches is a morphological parameter for predicting acute type B aortic dissection [4].

In addition to aortic arch type, other vascular properties such as tortuosity, angulation or loops in carotid arteries are sources of additional difficulties in endovascular navigation. In [5], it is shown that complex vascular anatomy, rather than age, is the risk factor behind CAS complication rate in patients over 80 years old. In mechanical thrombectomy, it is observed in [6] that tortuosity of extracranial CCA and internal carotid artery (ICA) influences time for accessing the occlusion site and radiation exposure time.

Considering all the above studies, knowing the type of aortic arch but also the anatomical specificities of the main afferent arteries provides crucial information to improve the navigation in complex cases. In fact, such prior knowledge can help physicians better plan their procedures and select the most appropriate catheter with respect to the patient's morphology.

The importance of vascular anatomy has motivated various contributions geared toward the analysis of geometrical features of vascular structures. In [7] an automated pipeline is based on anatomical landmarks for geometric characterization of the carotid siphon, an area in ICA responsible for several vascular pathologies. In [8], the geometry and deformation of the aortic arch vessels are quantified to characterize the effects of respiratory and cardiac motion on the origins of supra-aortic branches in the context of thoracic aortic aneurysms and dissections. More recently, in [6] a semiautomatic method is proposed to measure tortuosity and angulations of CCA and ICA to evaluate the effect of these geometric indicators on the performance of mechanical thrombectomy. Beyond these targeted studies that focused on the geometric characterization of vessels, more generic frameworks also propose sets of functions for geometric quantification of anatomical features, e.g. [9], [10].

Despite the importance of the geometry of the aortic arch and supra-aortic trunks, there is still a gap to fill for a complete characterization covering the entire catheter passage from the arch to the brain. In our previous work [11], we developed a deep learning segmentation pipeline from Magnetic Resonance Angiography (MRA) images to reconstruct the 3D volume of the aortic arch and its supra-aortic branches. Indeed, segmentation of vascular structures [12], [13] is a necessary prerequisite for geometry analysis and anatomical characterization. However, segmentation is not sufficient, and it must be followed by higher level image analysis procedures. For this reason and as an increment to our previous work [11], the scope of this article is oriented towards the proposal of an automatic vascular analysis approach that aims to evaluate, from 3D meshes, strategic anatomical / geometrical features: arch type, tortuosity, take-off angles, reverse curves, and other features quantifying the difficulty of navigation. This tool is dedicated to neuroradiologists to help them anticipate and better plan the endovascular procedures. The results have been quantitatively validated by experienced neuroradiologists at Rothschild Hospital (Paris, France) and have been used to document the First in Human study (registered with the French *Agence Nationale de Sécurité du Médicament et des produits de Santé* (ANSM) under the IDRCB number 2021-A02220-41-A) of the GECKO system, the *BCV* solution of a smart handle and active guidewire with shape-memory actuation control.

This article is organized as follows. The data used along with the proposed analysis framework and its settings are described in Sec. II. The results are presented and discussed in Sec. III. Conclusions and perspectives are given in Sec. IV.

II. MATERIAL AND METHODS

A. Data Acquisition and Preprocessing

A dataset[3] of 22 3T MRA volumes acquired on Philips imaging system (Ingenia 3T, Best, The Netherlands) using a 16 channels head coil was collected. These images were obtained from patients between 31 and 95 years old (avg. 72 years old, 59%/41% male/female).

The aortic arch and supra-aortic trunks to the carotid siphon were enhanced with a contrast agent for image acquisition monitored by bolus track injection technique. The acquisition parameters were as follows: coronal plane covering: 250 slices; active TR/TE $= 5.5/2.2$ ms; flip angle $= 27°$; number of excitations $= 1$; acquisition bandwidth = 476.7 Hz; FOV $= 380 \times 321$; voxel size = $0.5 \times 0.5 \times 1.0$ mm. The imaging time was 69 sec.

We performed the same preprocessing steps as in our previous work [11]. We resampled the MRA volumes to the isotropic resolution of $1.0 \times 1.0 \times 1.0$ mm and we homogenized their intensity distribution by normalizing the mean and standard deviation. In our case, the resampling does not affect the shape of the vessels. These spatial and signal normalizations were motivated by the deep learning framework underlying the proposed segmentation method.

B. Ground-Truth Data

All the 22 patients were 3D modeled using the pipeline from [11], leading to 3D meshes of vascular structures as output. The obtained 3D meshes were corrected (smoothing and area filtering) and validated by neuroradiologists of the Adolphe de Rothschild Foundation Hospital using the 3D Slicer software[4].

The aortic arch types of these volumes were assessed by three experienced neuroradiologists (RB, SE and RF). Because of inter-observer variability, especially between type II and III, a consensus by majority vote was considered to determine the ground-truth. Based on this human-expert analysis, types I, II, and III were observed in 27%, 18%, and 55% of patients, respectively.

The geometric feature ground-truth (tortuosity index, vessel length, and reverse curves) were also determined by neuroradiologists in a semi-automatic manner using PORTAL

[3]This dataset is the property of the Department of Neuroradiology of the Adolphe de Rothschild Foundation Hospital, Paris, France.

[4]https://www.slicer.org

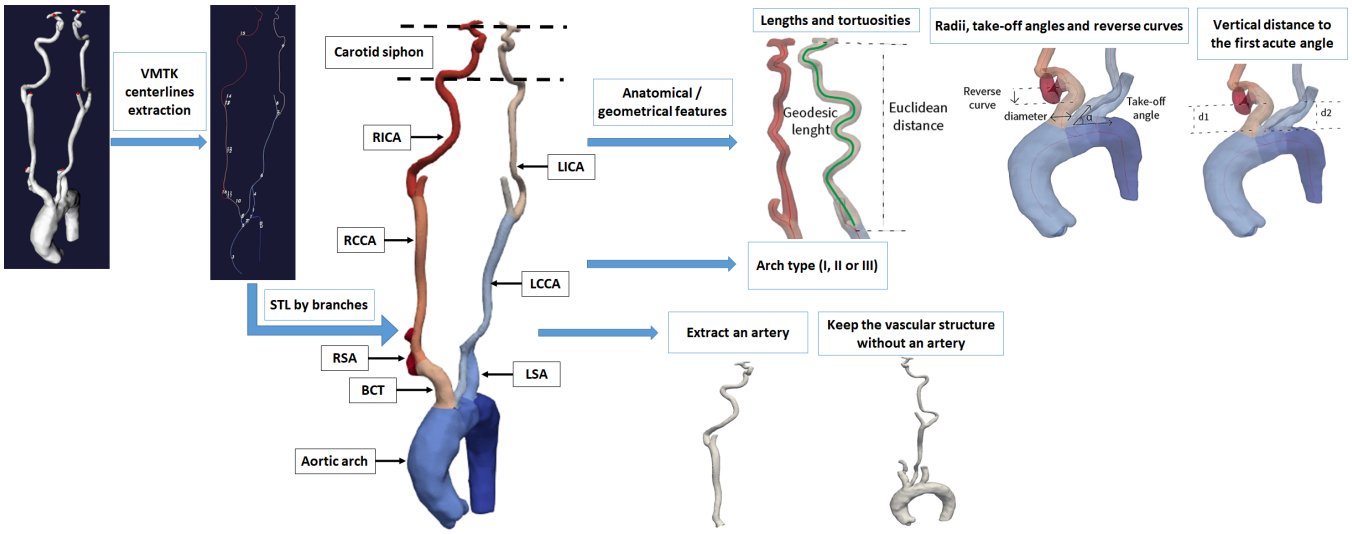

Fig. 2. Overview of the geometric characterization of the aortic arch and supra-aortic trunks: the centerlines of the meshes are used to classify the aortic arch, and calculate a set of anatomical/geometric features. All these indicators are calculated for each of the branches of the aortic arch and its supra-aortic trunks (STL branches). The framework also allows the extraction/removal of a specific artery for local anatomical characterization.

software (Ingenia Elition X, Philips Healthcare, Best, The Netherlands).

C. Automated Aortic Anatomy Analysis

For our anatomical analysis, the input data are the same 3D meshes as described in the previous section. In other words, at this stage, we no longer aim to evaluate the segmentation process [11], but we only focus on evaluating and automating the anatomy characterization of the aorta (aortic arch classification, geometric feature computation).

These input meshes represent the tubular architecture of the aortic arch and its supra-aortic trunks, which can be approximated by their centerlines. These centerlines of vessels are calculated using the Vascular Modeling Toolkit[5] (VMTK 1.4.0 under Python 3.6 and NVIDIA RTX 3090) which relies on the Voronoi diagram calculated using its dual Delaunay tessellation [9]. Based on neuroradiologists' recommendations, it was chosen to partition the centerlines into a subset of specific arteries done on the framework's graphical interface: the aortic arch, the left subclavian artery (LSA), the left common carotid artery (LCCA), the left internal carotid artery (LICA), and the brachiocephalic trunk (BCT) with its two bifurcations: the right subclavian artery (RSA) and the right common carotid artery (RCCA) with its bifurcation into the right internal carotid artery (RICA).

This partitioning then enables the extraction of the characteristics of specific arteries of interest, in addition to the global characteristics of the supra-aortic trunks. In particular, the anatomy analysis module depicted in Fig. 2 calculates a set of anatomical/geometrical features for each of the previously mentioned arteries. This set of features includes: arch type, artery lengths, radii at artery origin, tortuosity index, take-off angles, reverse curves as well as the vertical distance from the origin of supra-aortic trunks to the first acute angle. This extraction task is performed automatically once the anatomical analysis module is fed with 3D meshes.

Based on neuroradiologists expertise, these features were defined and formalized as follows, to best meet their needs:

- **Arch type (I, II or III)**: is determined by computing the average diameter of a 10 mm long segment of the LCCA, 20 mm away from its origin (indeed, radii at the origins are larger) and comparing it to the vertical distance between the origin of the brachiocephalic trunk and the apex of the aortic arch to apply the rule described in [1] (see also Fig. 1).
- **Artery lengths**: are calculated as the geodesic distance along the centerlines from the origin of the supra-aortic trunks to the carotid siphon. The lengths of the internal carotid arteries (LICA and RICA) are computed the same way, as well as the BCT.
- **Radii at artery origin**: the radius is calculated at the origin of each of the aforementioned arteries and bifurcations (by assuming a circular cross section of the arteries).
- **Tortuosity index**: following [14], this index is computed as the ratio between two distances: (1) the geodesic length along the centerline of the artery, and (2) the Euclidean distance between the two end-points of the artery segment. This index lies in $[1, +\infty)$: the closer to 1 the less tortuous. To improve the ability to assess the catheter navigation difficulty, two tortuosity indices were considered: a first for the overall tortuosity of the supra-aortic trunks to the carotid siphon; a second for the bifurcations in the internal carotids (LICA and RICA).
- **Take-off angles**: is the angle formed between a supra-aortic trunk (LCCA or BCT) and the aortic arch. Following [8], this angle is determined by two vectors starting at the ostium and ending 10 mm further, oriented

[5]http://www.vmtk.org

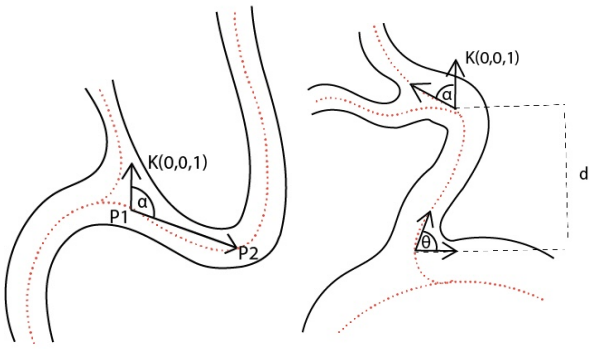

Fig. 3. Reverse curve on the left ($\alpha \geq 100°$ between the 5 mm long vector $\overrightarrow{P_1P_2}$ and the unit vector $\overrightarrow{K}$ in the direction of the Z axis). On the right, the vertical distance from the origin of supra-aortic trunk to the first acute angle ($\alpha \geq 45°$ and θ a take-off angle).

TABLE I

RESULTS OF AORTIC ARCH CLASSIFICATION. COMPARISON BETWEEN CLINICAL GROUND-TRUTH AND AUTOMATED MEASURES.

Arch type	Precision	Recall	F1-score
Type I	1.00	1.00	1.00
Type II	0.80	1.00	0.89
Type III	1.00	0.92	0.96

TABLE II

RESULTS OF LENGTHS AND TORTUOSITIES. COMPARISON BETWEEN CLINICAL AND AUTOMATED MEASURES. THE ABBREVIATION RCCA (RESP. LCCA) HERE INCLUDES THE ENTIRE ARTERY UP TO THE CAROTID SIPHON.

Artery	Length			Tortuosity		
	Pearson	RMSE	MAPE	Pearson	RMSE	MAPE
RCCA	0.97	5.97	1.75	0.93	0.06	3.32
LCCA	0.92	6.80	1.74	0.95	0.04	2.30

along the centerlines of the arch and the supra-aortic trunk, respectively.

- **Reverse curve (a.k.a. turning point)**: is an indicator of how many times the tortuosity of the artery leads to reverse the direction of the catheter along its path. (In such case, the physician needs to reverse the catheter from its vertical direction by lowering it in order to access the rest of the artery). The supra-aortic centerline is sampled into successive segments of 5 mm length. For each of these segments, the angle is computed with respect to the vertical direction (Z axis). If an angle is greater than or equal to $100°$, then a reverse curve is detected (see Fig. 3, left). Reverse curves are determined in LCCA, RCCA and their respective bifurcations into LICA and RICA.
- **Vertical distance from the origin of supra-aortic trunks to the first acute angle**: this indicator aims to quantify the navigation difficulty at the origin of supra-aortic trunks by calculating the distance d between the loci of two acute angles: the first angle, at the origin of the supra-aortic trunk, is a take-off angle (calculated previously); the second, located on the same centerline, is an acute angle if the artery is deviated more than $45°$ from the vertical trajectory (Fig. 3, right). These angles are calculated the same way as described above (see Take-off angles). The lower the distance d, the more difficult to access after engaging the ostium of a supra-aortic trunk.

III. RESULTS AND DISCUSSION

The anatomical / geometrical features described above were validated by experienced neuroradiologists. As stated in Sec. II-B, a series of measurements were performed by these human experts on 22 patients. These ground truth measurements were compared with those automatically provided by the strategy described in Sec. II-C.

A. Arch Type Classification

Usually, the arch type is determined visually based on the elongated appearance of the arch and the tortuosity of the supra-aortic trunks. In our case, the Madhwal [1] rule was implemented and compared with the majority vote consensus of three experienced neuroradiologists (RB, SE and RF). In this context, the Pearson correlation coefficient between the clinical and automated results was 97% with 95% of accuracy. To properly measure the quality of the arch classification, we calculated the precision, recall, and F1-score, provided in Tab. I, from the induced multiclass confusion matrix.

We noted one misclassification: a patient whose arch type according to clinicians was predominantly classified as type III compared with the automated result where type II was assigned. In fact, the problem of misclassification between type II and III arches is common among clinicians since classification is usually estimated visually. Thus, the automation of this indicator makes it possible to better estimate the type, enabling to anticipate the difficulty of navigation and to choose the most adapted catheter to the morphology of the patient.

B. Geometrical Features

For the length and tortuosity features, we validated our results on the two supra-aortic arteries: RCCA and LCCA to the carotid siphon. In this context, Pearson correlation coefficient, root mean squared error (RMSE) and mean absolute percentage error (MAPE) were calculated, see Tab. II. For the RCCA (resp. LCCA) to the carotid siphon, we noted 5.97 mm (resp. 6.80 mm) average difference between automatic and clinical lengths, and 0.06 (resp. 0.04) average difference between automatic and clinical tortuosity indices. This slight difference—less than 2% error for lengths and around 3% for tortuosities—can be explained by the selection points (inlets and outlets) for the measurements performed by the neuroradiologists. In addition to what is shown in Tab. II, details of the lengths and tortuosities for LICA and RICA can also be extracted individually.

Similarly to the arch type, the number of reverse curves is usually estimated visually from the MRA volumes, which can sometimes be difficult due to noise and motion artifacts.

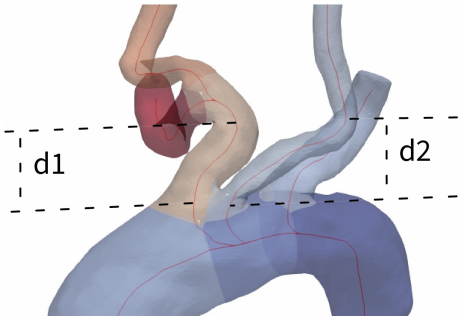

Fig. 4. Access difficulty in BCT and LCCA. Acute angles forming sharp bends at small vertical distances (d_1 and d_2) before engaging the supra-aortics trunks.

We compared the measurements obtained from the characterization module with clinical observations. We found that the number of reverse curves from RCCA (resp. LCCA) to carotid siphon has a Pearson coefficient of 0.88 (resp. 0.96). In particular, for RCCA the number of reverse curves was incorrectly predicted in three patients, compared with only one patient for LCCA. With our characterization tool, reverse curves are detected before and after the bifurcation into internal and external carotids.

Indicators such as radii at the origin of supra-aortic trunks and take-off angles were calculated but not yet validated because of the absence of clinical measurements. These manual measurements are being collected for a broader evaluation. This is also the case for the vertical distance between the origin of supra-aortic trunks and the first acute angle. Nonetheless, a qualitative validation was performed by neuroradiologists. Patients with a small vertical distance obtained with the characterization module were reviewed by physicians to confirm the access difficulty (see Fig. 4).

IV. CONCLUSION AND PERSPECTIVES

This paper proposes an automatic analysis of anatomical and geometrical features related to the aortic arch and supra-aortic trunks. Our framework is fed with meshes obtained from CNN-based vascular segmentation, leading to a complete analysis pipeline, from MRA images to high-level features: arch type, tortuosities, reverse curves, take-off angles and access difficulty after engaging an artery. These features were validated by physicians at the hospital.

Our aim is to help neuroradiologists anticipate the navigation difficulties during endovascular procedures. To reach that goal, this work could be improved by characterizing the carotid siphon, which is a complex area responsible for several vascular pathologies. Other features describing severe angulation of arteries could also be investigated such as kinking, looping and coiling. A wider clinical validation of our features on a diversified dataset in terms of demographic, pathological and imaging data of different modalities and resolutions is also planned.

V. COMPLIANCE WITH ETHICAL STANDARDS

This research study was conducted retrospectively using human patients' data. An oral and written information about image post-processing was delivered. The study was approved by the Institutional Ethical Committee in accordance with the 1964 Helsinki declaration and its later amendments. Written consent was waived.

ACKNOWLEDGMENT

The authors acknowledge the *Fondation Adolphe de Rothschild hospital* for the clinical MR images used in this research and the neuroradiologists R. Blanc (RB), M. Piotin (MP), S. Escalard (SE) and R. Fahed (RF) for the clinical validation of our results.

REFERENCES

[1] S. Madhwal, V. Rajagopal, D. L. Bhatt, C. T. Bajzer, P. Whitlow, and S. R. Kapadia, "Predictors of difficult carotid stenting as determined by aortic arch angiography," *J Invasive Cardiol*, vol. 20, pp. 200–204, 2008.

[2] F. Burzotta, R. Nerla, G. Pirozzolo, C. Aurigemma, G. Niccoli, A. M. Leone, S. Saffioti, F. Crea, and C. Trani, "Clinical and procedural impact of aortic arch anatomic variants in carotid stenting procedures," *Catheter Cardio Inte*, vol. 86, pp. 480–489, 2015.

[3] S. Shen, X. Jiang, H. Dong, M. Peng, Z. Wang, W. Che, Y. Zou, and Y. Yang, "Effect of aortic arch type on technical indicators in patients undergoing carotid artery stenting," *J Int Med Res*, vol. 47, pp. 682–688, 2019.

[4] L. Sun, J. Li, Z. Liu, Q. Li, H. He, X. Li, M. Li, T. Wang, L. Wang, Y. Peng, H. Wang, and C. Shu, "Aortic arch type, a novel morphological indicator and the risk for acute type B aortic dissection," *Interact Cardiovasc Thorac Surg*, vol. 34, pp. 446–452, 2022.

[5] A. A. Fanous, P. K. Jowdy, S. Morr, K. Vakharia, H. Shallwani, K. Lorincz, L. N. Hopkins, J. M. Davies, K. V. Snyder, A. H. Siddiqui, and E. I. Levy, "Vascular anatomy and not age is responsible for increased risk of complications in symptomatic elderly patients undergoing carotid artery stenting," *World Neurosurg*, vol. 128, pp. e513–e521, 2019.

[6] M. Mokin, M. Waqas, F. Chin, H. Rai, J. Senko, A. Sparks, R. W. Ducharme, M. Springer, C. V. Borlongan, E. I. Levy, C. Ionita, and A. H. Siddiqui, "Semi-automated measurement of vascular tortuosity and its implications for mechanical thrombectomy performance," *Neuroradiology*, vol. 63, pp. 381–389, 2021.

[7] H. Bogunović, J. M. Pozo, R. Cárdenes, M. C. Villa-Uriol, R. Blanc, M. Piotin, and A. Frangi, "Automated landmarking and geometric characterization of the carotid siphon," *Med Image Anal*, vol. 16, pp. 889–903, 2012.

[8] G.-Y. Suh, R. E. Beygui, D. Fleischmann, and C. P. Cheng, "Aortic arch vessel geometries and deformations in patients with thoracic aortic aneurysms and dissections," *J Vasc Interv Radiol*, vol. 25, pp. 1903–1911, 2014.

[9] M. Piccinelli, A. Veneziani, D. A. Steinman, A. Remuzzi, and L. Antiga, "A framework for geometric analysis of vascular structures: Application to cerebral aneurysms," *IEEE Trans Med Imaging*, vol. 28, pp. 1141–1155, 2009.

[10] H. A. Kjeldsberg, A. W. Bergersen, and K. Valen-Sendstad, "morphMan: Automated manipulation of vascular geometries," *J Open Source Soft*, vol. 4, pp. 1065, 2019.

[11] M. Lahlouh, Y. Chenoune, R. Blanc, J. Szewczyk, and N. Passat, "Aortic arch anatomy characterization from MRA: A CNN-based segmentation approach," in *IEEE ISBI*. IEEE, 2022, pp. 1–5.

[12] D. Lesage, E. D. Angelini, I. Bloch, and G. Funka-Lea, "A review of 3D vessel lumen segmentation techniques: Models, features and extraction schemes," *Med Image Anal*, vol. 13, pp. 819–845, 2009.

[13] S. Moccia, E. De Momi, S. El Hadji, and L. S. Mattos, "Blood vessel segmentation algorithms - Review of methods, datasets and evaluation metrics," *Comput Methods Programs Biomed*, vol. 158, pp. 71–91, 2018.

[14] S. Ciurică, M. Lopez-Sublet, B. L. Loeys, I. Radhouani, N. Natarajan, M. Vikkula, A. H. E. M. Maas, D. Adlam, and A. Persu, "Arterial tortuosity: Novel implications for an old phenotype," *Hypertension*, vol. 73, pp. 951–960, 2019.